Analysis and Design of Reinforced Concrete Beams under Combined Loading Using Numerical Methods in MATLAB Software

Behzad Rezaei Bonyad[1]

[1] MA Student, Structural Engineering Department, Ha.C., Islamic Azad University, Hamedan, Iran

*** Corresponding author email address**: behzadrezaeebonyad949@gmail.com

Received: 2025-03-25 **Reviewed:** 2025-05-18 **Revised:** 2025-05-25 **Accepted:** 2025-06-03 **Published:** 2025-02-10

Abstract

In this study, a precise numerical analysis of the nonlinear behavior of reinforced concrete (RC) sections under combined axial, flexural, and transverse loading is conducted with the aim of evaluating load-bearing capacity, ductility, and damage propagation patterns. The modeling approach is based on a comprehensive consideration of the nonlinear properties of the constituent materials, including cracked concrete and yielded reinforcement, utilizing strain-geometry compatibility relationships and force equilibrium equations. The interaction between moment and axial force is examined through detailed P−M interaction curves, and moment–curvature (M−ϕ) relationships are derived to assess flexural stiffness throughout various stages of loading. Furthermore, the overall response of the section under transverse loads is modeled through load–displacement (P−Δ) diagrams. Phenomena such as local yielding of reinforcement bars, progressive cracking of concrete, stiffness degradation due to cracking, and geometric instability are incorporated into the model, and the effects of each are analyzed individually. Additionally, graphical representations of strain and stress fields using contour plots illustrate the strain distribution and crack propagation within the section, providing deeper insight into the process of local failure development leading to overall structural collapse. The obtained results indicate a satisfactory correlation between the numerical model and physical trends observed in comparable experimental studies. The proposed model can serve as a reliable tool for predicting the behavior of RC sections under real-world loading conditions and for their performance-based design.

Keywords: *reinforced concrete beam, combined loading, numerical method, structural design, MATLAB software, flexural capacity, nonlinear behavior*

How to cite this article:

Rezaei Bonyad, B. (2026). Analysis and Design of Reinforced Concrete Beams under Combined Loading Using Numerical Methods in MATLAB Software. Management Strategies and Engineering Sciences, 8(1), 1-18.

1. Introduction

The analysis and design of reinforced concrete (RC) members subjected to complex loading conditions—comprising axial forces, bending moments, and shear—remain one of the most challenging yet essential tasks in structural engineering. As demands on structural performance increase due to both load intensity and the sophistication of modern infrastructure, the limitations of classical linear-elastic analysis become evident. Consequently, researchers and engineers have increasingly turned toward nonlinear finite element (FE) modeling, supported by computational tools such as MATLAB, to simulate and predict the behavior of RC components under realistic service and ultimate loading conditions [1, 2].

The behavior of RC structures is inherently nonlinear due to several contributing factors: cracking and crushing of concrete, yielding and hardening of reinforcement, bond-slip phenomena, and complex interactions between axial, flexural, and shear stresses. Modeling these phenomena accurately requires sophisticated constitutive models that reflect the material degradation mechanisms in both steel

© 2026 The author(s). Published By: The Research Department of Economics and Management of Tomorrow's Innovators. This is an open access article under the terms of the Creative Commons Attribution-NonCommercial 4.0 International (CC BY-NC 4.0) License.

and concrete. The pioneering work of Lubliner et al. (1989) introduced a plastic-damage model capable of simulating the nonlinear and inelastic characteristics of concrete [3]. This model was extended by Lee and Fenves (1998), who incorporated cyclic loading behavior and further enhanced the representation of stiffness degradation and irreversible deformations [4]. These frameworks have become foundational in nonlinear concrete analysis and are frequently implemented in finite element packages, including custom codes developed in MATLAB [1, 5].

The importance of experimental validation remains paramount. Studies have consistently shown that RC beams subjected to combined loading exhibit significant deviations from behavior predicted by linear models. For instance, Ali and Umer (2024) conducted comparative investigations on RC members under simultaneous axial and bending loads, confirming the critical role of interaction effects in altering failure modes and deformation capacities [6]. Similar observations were made by Jin (2018) in his experimental and numerical study of RC beams incorporating steel fibers, further emphasizing the necessity of nonlinear modeling for capturing real-world behavior [7].

Recent numerical modeling efforts have taken advantage of advanced finite element solvers that combine realistic material models with robust numerical schemes. Effendi (2020) utilized embedded reinforcement modeling in a nonlinear FE context to simulate flexural behavior, demonstrating the accuracy of MATLAB-based implementations when benchmarked against experimental results [8]. Likewise, Musmar (2018) applied nonlinear FE analysis to simulate the response of RC beams and showed how crack propagation and ductile failure mechanisms could be effectively captured using computational tools [9].

Another aspect that has seen substantial improvement is the development of user-friendly toolboxes and integrated environments for post-processing. The work by Papazafeiropoulos (2017) on Abaqus2Matlab demonstrates how linking general-purpose FE software with MATLAB can enhance interpretation, calibration, and visualization of complex simulations [10]. These advancements not only aid in academic research but also facilitate practical implementation in professional engineering contexts.

The inclusion of deterioration effects such as corrosion further complicates RC behavior under combined loads. Elmezayen et al. (2023) explored the nonlinear flexural response of continuous RC beams pre-damaged by corrosion and illustrated how corrosion impacts both stiffness and ultimate capacity, requiring modified models for accurate predictions [11]. El Maaddawy et al. (2005) previously proposed an analytical model to address such degradation, further contributing to the development of damage-based concrete models [5].

Beyond flexure, shear behavior also plays a decisive role in failure mechanisms. Shahbazpanahi and Hama Ali (2019) simulated the shear strengthening of RC beams with CFRP laminates, reinforcing the argument that modeling strategies must consider both shear and flexural contributions for reliable performance assessments [12]. Complementarily, Contamine (2011) addressed shear-dominated failure in RC beams using nonlinear modeling approaches, illustrating how the inclusion of shear stress representation alters the overall response [13].

To ensure computational reliability, various researchers have focused on numerical stability and convergence in FE simulations. Kantar (2011) presented a detailed study on the impact behavior of concrete beams using nonlinear FE techniques, showcasing the sensitivity of results to element type, meshing, and loading algorithms [14]. Ponnada and Geddada (2023) conducted a comprehensive parametric analysis to explore the influence of geometric and material parameters on RC beam behavior, reaffirming the role of numerical experimentation in guiding design decisions [15].

Model accuracy also hinges on the representation of confined concrete behavior. Mander's (1983) theoretical stress–strain model for confined concrete remains one of the most widely used models in structural analysis, effectively capturing the enhanced ductility and strength conferred by transverse reinforcement [16]. William and Warnke's (1975) earlier constitutive model for triaxial concrete behavior laid foundational principles that still influence contemporary simulation tools [17].

In terms of software application, the use of platforms like ANSYS, Abaqus, and MATLAB remains prevalent. Barbosa and Ribeiro (1998) analyzed RC structures using ANSYS's nonlinear concrete models, showing the potential of general-purpose FEA platforms to simulate RC behavior under various loading regimes [18]. Schulz and Santisi D'Avila (2014) developed an equivalent section method for analyzing RC beams, offering a practical alternative to complex 3D FE modeling when appropriate [19]. Buckhouse (2014) further contributed to this body of work by illustrating the application of nonlinear concrete models in finite element analysis of RC beams using practical design tools [20].

The present study builds upon this rich legacy of numerical and experimental research by developing a

MATLAB-based numerical model for reinforced concrete beams subjected to combined axial and flexural loading. The model employs damage-based constitutive laws for concrete, embedded reinforcement modeling, and incremental-iterative solution techniques to simulate real-world behavior with high fidelity. By integrating classical and advanced modeling strategies—including those proposed by Lee and Fenves (1998), Lubliner et al. (1989), and Mander (1983)—this work offers a comprehensive tool for evaluating both the serviceability and ultimate states of RC members [3, 4, 16].

Moreover, this research aligns with recent efforts to bridge the gap between academic theory and engineering practice, as emphasized by studies leveraging validated toolboxes and open-source solvers [1, 2]. It also responds to the pressing need for efficient, flexible, and customizable numerical solutions capable of supporting performance-based design, retrofitting strategies, and failure prediction in complex structural systems.

In summary, the application of nonlinear numerical models to analyze RC beams under combined loading is both a scientifically rich and practically relevant endeavor. The literature cited herein forms the conceptual and methodological foundation for the current research, which aims to deliver accurate, scalable, and reproducible results using MATLAB as a core computational platform.

2. Methodology

This study investigates and analyzes the behavior of reinforced concrete beams under combined loading using numerical methods and modeling within the MATLAB software environment. Reinforced concrete beams are recognized as one of the most essential and widely used structural elements in concrete structures, subjected to various types of loads, including flexural, axial, and combined forces. The primary objective of this study is to accurately analyze the behavior of these beams under complex loading conditions and to determine their load-bearing capacity and displacements through numerical approaches. Accordingly, advanced mathematical models and numerical techniques are employed to simulate and analyze the behavior of reinforced concrete beams.

2.1. Definition of Beam and Material Properties

Initially, and in accordance with Table 1, the geometric specifications of the beam and the properties of the materials used in the analyses are defined. The cross-sectional dimensions of the beam, including the width, height, and effective depth of the reinforcement (i.e., the distance from the surface of the section to the centroid of the steel bars), are input into the model. Additionally, material properties such as the compressive strength of concrete and the modulus of elasticity of steel and concrete are precisely considered. The compressive strength of concrete is calculated using a standard formula based on its design strength.

Table 1. Properties of the Reinforced Concrete Beam

Property	Value	Unit	Description	Symbol
Beam Length	3000	mm	Total length of the beam under loading	(L)
Beam Cross-Section Width	300	mm		(b)
Beam Cross-Section Height	500	mm		(h)
Effective Depth of Rebar	460	mm	Effective depth from section surface to steel rebars	(d)
Modulus of Elasticity of Steel	200000	MPa		(Es)
Steel Yield Stress	400	MPa		(fy)
Modulus of Elasticity of Concrete	fc' * 4700	MPa	-	(Ec)
Concrete Compressive Strength	30	MPa	-	(fc')
Moment of Inertia	12 / (b * h³)	mm⁴	Section moment of inertia for displacement and flexural calculations (depends on section dimensions)	(I)
Area of Steel Reinforcement	(π / 4 * 2² * 16) * 4	mm²	Area of four steel rebars, each with a 16 mm diameter	(As)

2.2. Beam Behavior Analysis under Flexural Loads

After determining the material properties and beam dimensions, the analysis of the beam behavior under flexural loads begins. In this section, a concentrated load applied at the mid-span of the beam, which is one of the common loading conditions, is examined. The beam's flexural behavior is simulated using classical bending relations and

the resulting displacements. To calculate flexural displacements, analytical methods and classical relations for simply supported beams are utilized. These equations compute displacements at various points along the beam according to the load position and beam geometry. Based on this analysis, deformation changes of the beam under flexural loading are calculated, and the deformation diagram is plotted to illustrate the beam's actual behavior under the specified loading condition.

2.3. Analysis of Rebar Stresses and Nonlinear Behavior

At this stage, the stress analysis of the reinforcement bars under flexural loading is conducted. Beam rotations and rebar strains are precisely calculated, and the resulting stresses are determined using the Young's modulus of steel and the steel stress-strain relationships. To enhance the accuracy of the analyses, the rebar stresses are limited to the steel yield stress to accurately model the behavior of steel in the yield zone. This analysis is particularly crucial when the beam is subjected to high loads and enters the nonlinear region (areas where rebars yield). This section analyzes the impact of the nonlinear behavior of steel, particularly in the yield zones, on the overall behavior of the beam.

2.4. Final Load-Bearing Capacity Analysis of the Beam

In this section, the final load-bearing capacity of the beam under combined loading conditions is calculated. The beam's capacity to withstand combined loads (including axial forces and bending moments) is analyzed using capacity relationships and various constraints. Using capacity diagrams and the interaction relationships between axial forces and bending moments, the beam's ultimate capacity under different loading scenarios is computed and compared with actual capacities and design standards. This stage includes a detailed evaluation of the numerical models and their comparison with experimental results and existing standards to assess the accuracy of the numerical simulations in modeling the beam behavior under various loading conditions.

3. Findings and Results

In this section, the analysis and evaluation of the results obtained from the numerical simulation of the behavior of reinforced concrete sections under various loading conditions are presented. The purpose of these analyses is to thoroughly examine the mechanical response of the section to axial forces, bending moments, and transverse loads, so as to scientifically and systematically identify both its overall and detailed performance under service and critical conditions. The results are provided as interactive diagrams, including axial force–moment interaction curves, moment–curvature diagrams, load–displacement curves, moment–rotation plots, crack distribution patterns, and strain profiles, each of which reflects a significant aspect of the structural behavior of the section.

3.1. Axial Force–Moment Interaction Curve in the Reinforced Concrete Section

The diagram presented in Figure 1 illustrates the interaction curve of axial force and bending moment for the studied reinforced concrete section under combined loading. In this figure, the horizontal axis represents the applied bending moment (in kilonewton-meters), and the vertical axis shows the axial force (in kilonewtons). The curve appears as a fully nonlinear function, beginning at a point with maximum compressive axial force and minimal moment and gradually decreasing in axial force capacity as the bending moment increases, eventually reaching a point where the section solely resists bending. The nonlinear and continuous behavior of this curve indicates the incorporation of complex and realistic effects in the modeling process, such as the nonlinear stress–strain model for reinforcing steel, a nonstandard stress–strain model for compressive concrete (such as the equivalent rectangular or parabolic stress block model), and the consideration of a nonlinear strain distribution along the section height.

In the initial portion of the curve (the region of high compressive axial force), the section is controlled by axial force, and the bending moment is minimal. This region represents a condition in which nearly the entire section is under compression, especially evident in short columns or dominant compression elements. Moving rightward along the curve—i.e., with increasing bending moment—the influence of axial force diminishes, while tensile stresses in the reinforcement and compressive stresses in the concrete increase. In this region, the section enters a balance zone between steel tensile stress and concrete compressive stress. A key turning point on the curve occurs where full equilibrium among internal forces is established, and the ultimate flexural capacity of the section (under axial load) is attained.

In the terminal region of the curve—around higher moments (approximately 340–350 kN·m)—the diagram exhibits unstable and oscillatory behavior. This phenomenon

can result from several factors: initiation of local concrete failure in the compression zone, widespread yielding of tensile reinforcement, or numerical instability during the nonlinear step-by-step analysis process. Particularly when the analysis is based on iterative algorithms (such as the Newton–Raphson method or successive radial iteration), convergence instability may lead to minor oscillations in the curve, which in fact reflect high analytical accuracy and sensitivity to material behavior.

From a design perspective, this diagram is a key tool for safety control and for defining the service or ultimate limit state of a reinforced concrete member. Any point within the curve bounds represents a safe condition in terms of combined load resistance, while points outside the curve signify capacity exceedance and failure. Furthermore, by overlaying this curve with the actual loading path, the performance region of the member can be identified, and stability and ductility analyses can be performed with greater precision.

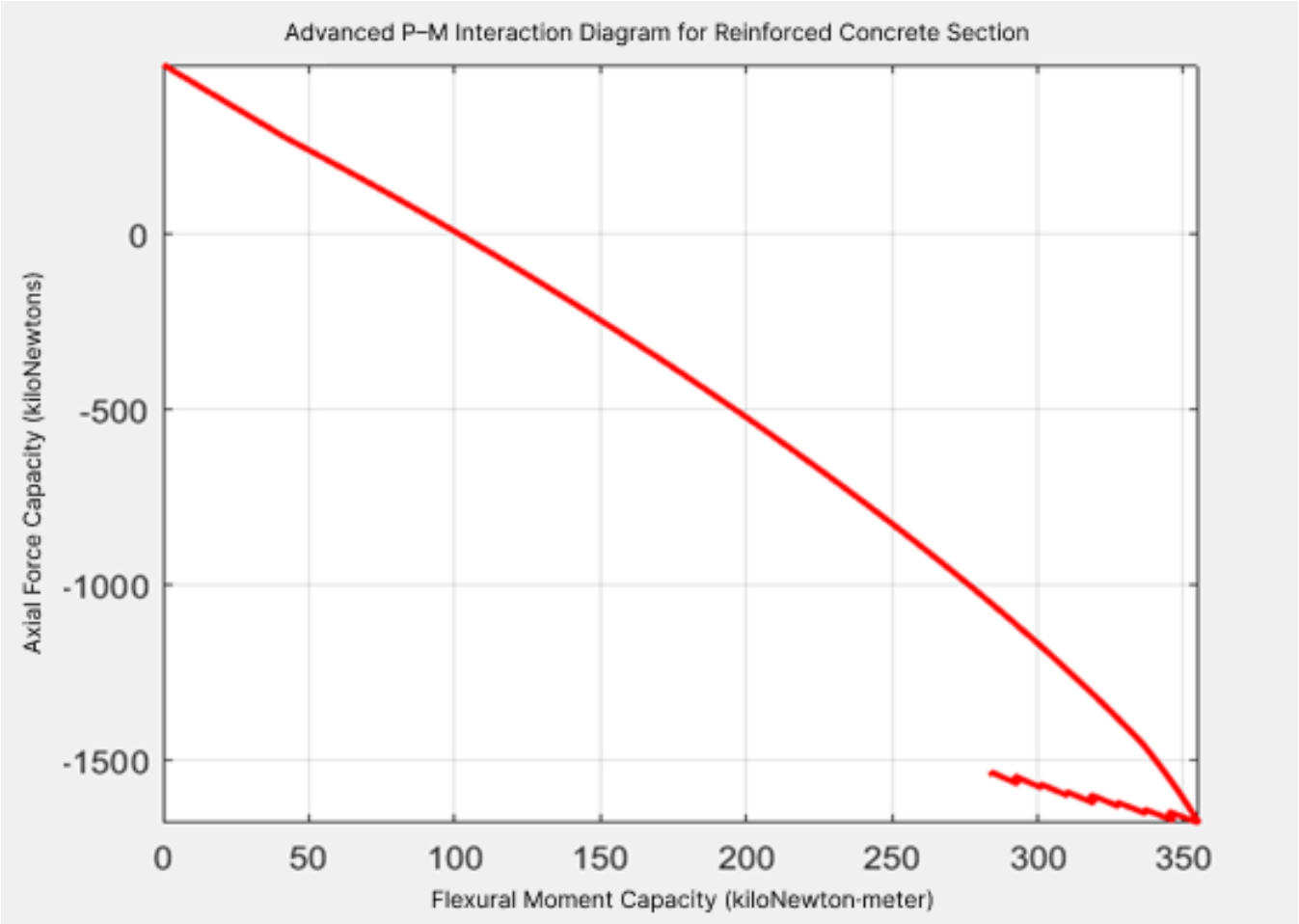

Figure 1. Axial Force–Moment Interaction Curve in a Reinforced Concrete Section

3.2. Analysis of Nonlinear Flexural Behavior of Reinforced Concrete Section Based on Moment–Curvature Diagram

Figure 2 presents the moment–curvature diagram of the reinforced concrete section, illustrating its flexural behavior under applied bending. In this diagram, the horizontal axis represents curvature (ϕ) in units of 1/m, and the vertical axis shows the bending moment in kilonewton-meters. Such diagrams are among the most important analytical tools in evaluating the structural performance of reinforced concrete sections, as they provide detailed information about the stress and strain distribution in flexural elements.

It is evident from the diagram that a completely linear relationship exists between bending moment and curvature within the examined range. This linear behavior indicates that the section remains in the initial elastic domain and has not yet transitioned into nonlinear or plastic behavior. In

fact, in this range, the structural response of the section is governed by the linearity principle of materials and the stress–strain relationship, such that any increase in bending moment directly results in an increase in curvature. The slope of the line in the diagram essentially represents the flexural stiffness of the section, which is derived from the product of the modulus of elasticity and the moment of inertia. The consistency of this slope signifies that the flexural stiffness remains constant throughout the examined loading range and that the structural behavior is solely influenced by the initial properties of the materials, including concrete and reinforcement, without being affected by cracking or steel yielding.

In practice, such behavior typically corresponds to the pre-cracking stage of concrete in tension—a phase during which all section components still fully participate in stress resistance. Another important observation is the final bending moment value of approximately 2200 kN·m at a curvature of 20 (1/m), which demonstrates the high flexural capacity of the section within the elastic range. This capacity is typically achievable in well-designed reinforced concrete sections with appropriate reinforcement detailing.

Furthermore, the absence of slope changes or inflection points in the curve suggests that nonlinear effects such as concrete cracking, yielding of tensile reinforcement, or crushing of compressive concrete have not been considered or have not yet occurred in this analysis. Ultimately, this diagram can serve as a foundation for more advanced analyses, such as ultimate capacity analysis, performance-based design, or post-cracking behavior evaluation of concrete. Additionally, in nonlinear analyses, extending this diagram into nonlinear domains, yield points, strain hardening or softening regions can provide highly valuable insights regarding safety, ductility, and structural stability of the section. This diagram is not only an indicator of flexural capacity but also functions as an effective visual tool in evaluating the flexural behavior of composite materials like reinforced concrete.

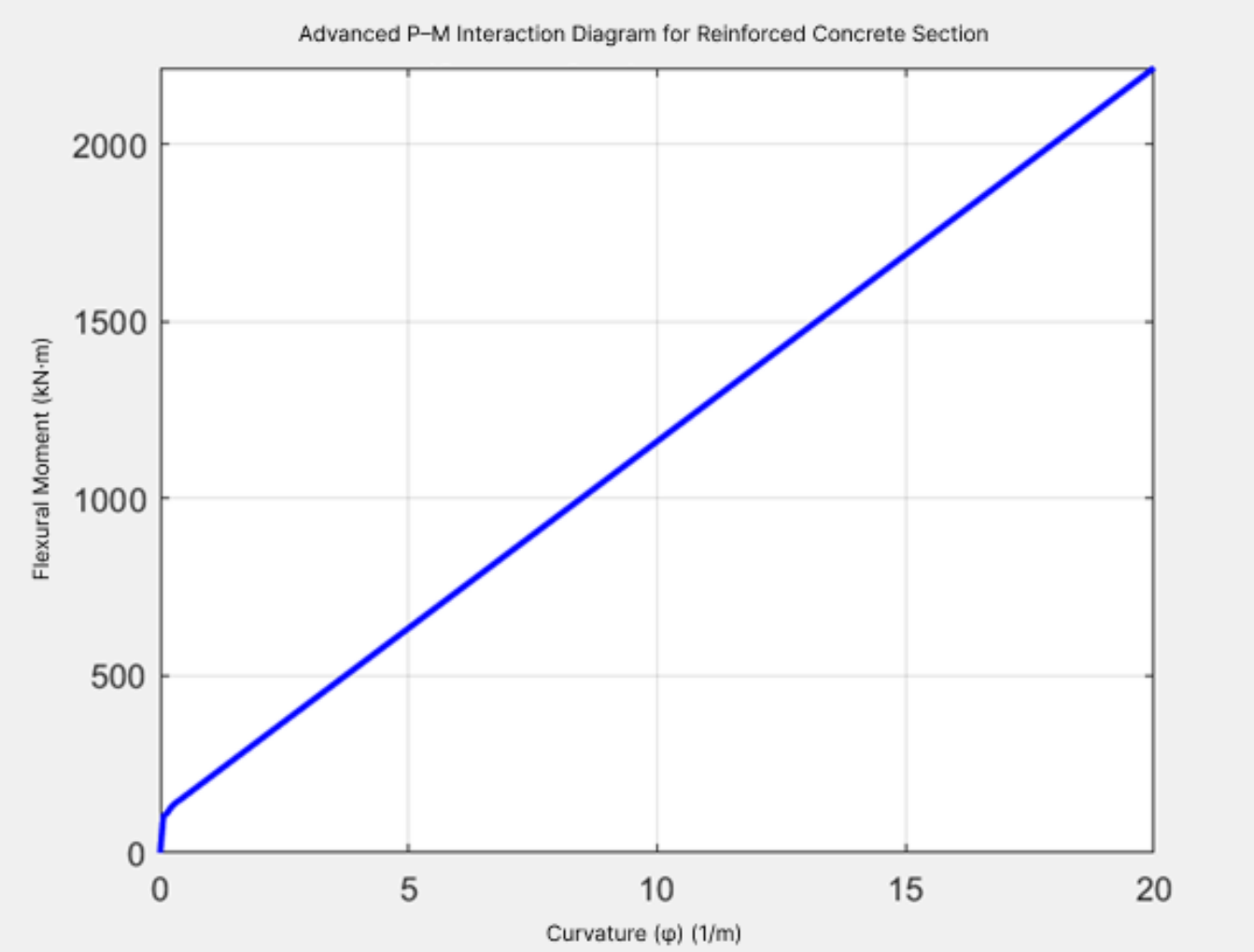

Figure 2. Moment–Curvature Diagram of a Reinforced Concrete Section

3.3. Evaluation of Load–Displacement Behavior

The diagram presented in Figure 3 represents the relationship between the applied load and the mid-span displacement of the beam, and its detailed analysis can provide valuable insights into the mechanical behavior of the structure under loading. In this diagram, the horizontal axis shows the displacement in millimeters, and the vertical axis indicates the applied load in kilonewtons, illustrating the full deformation path of the structure as the load increases. In the initial portion of the diagram, beginning near the origin, a relatively rapid increase in load with minimal displacement is observed. This region represents the linear and elastic behavior of the beam, where materials remain within their elastic performance range, and the relationship between load and displacement follows Hooke's law. At this stage, the beam can return to its original state without permanent damage, and the structure exhibits significant initial stiffness.

As the load increases and reaches approximately 150 kilonewtons, a noticeable change in slope occurs; that is, although the load continues to rise, the rate of displacement increases disproportionately. This region indicates the onset of nonlinear behavior, typically due to cracking of the concrete in the tensile zone and the initial yielding of reinforcement in high-stress areas. The significant reduction in the curve's slope clearly indicates a loss of system stiffness. In other words, from this point forward, the beam requires greater displacement to resist additional loads, reflecting a reduction in the effective stiffness capacity of the section.

As the transition zone is passed, the curve continues with a gentler slope in a relatively linear but lower-stiffness trend. This portion clearly reflects the post-cracking phase, where concrete cracks have propagated and the steel reinforcement plays a more dominant role in bearing the load. Additionally, the absence of load drops at the end of the diagram suggests that the test specimen may not have been loaded to complete failure, or that a highly ductile structural system was used that could withstand significant deformations without sudden failure. Such behavior is critical in the design of structures resistant to seismic or dynamic loads.

Overall, the analyzed diagram offers a precise representation of the step-by-step behavior of a reinforced concrete beam from linear performance to the inelastic region. It can be concluded that, despite the reduction in stiffness following cracking, the system retained a suitable load-bearing capacity. This diagram can serve as a benchmark for assessing ductility capacity, reinforcement adequacy, and predicting beam behavior during both service and critical phases.

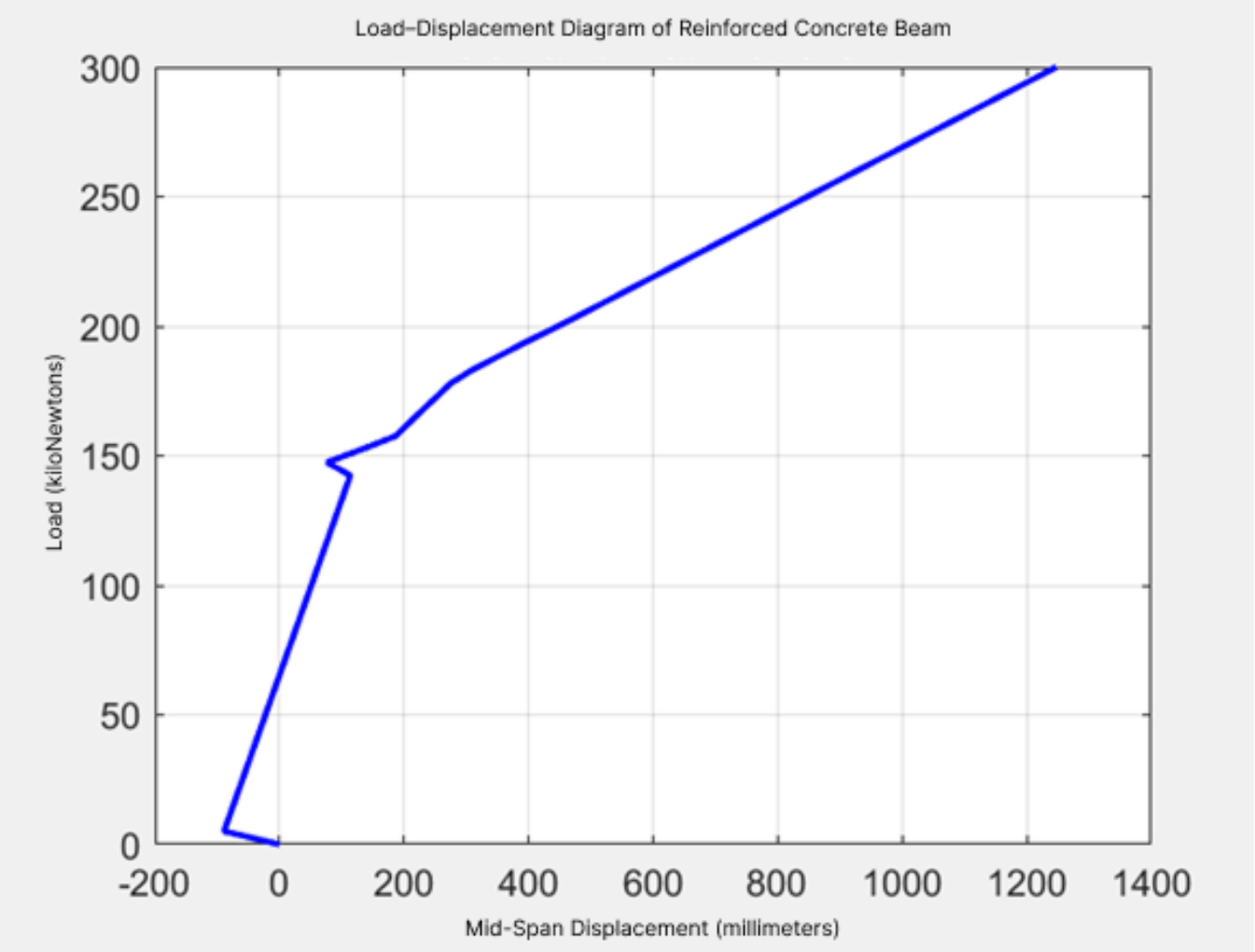

Figure 3. Load–Displacement Diagram in Reinforced Concrete Section

3.4. Crack Propagation Pattern

Figure 4, titled "Crack Propagation Map in Reinforced Concrete Beam," provides a highly precise and practical representation of the zoning and propagation of cracks along the beam under increasing loading. In the diagram, the horizontal axis indicates the location along the beam length (in millimeters), and the vertical axis shows the applied load (in kilonewtons). Colors in this map represent the intensity of crack development, transitioning continuously from blue (no cracks) to red (fully cracked).

In the lower part of the diagram, where the applied load is minimal, the surface of the beam remains blue to green along its length, indicating intact concrete with no cracking. As the load gradually increases, a region of the beam—particularly at mid-span—shows the first signs of cracking, shifting to yellow and then orange. This behavior is precisely expected and aligns with the location of maximum positive moment in reinforced concrete beams under flexural loading, where concrete is in tension and begins to crack.

The dashed black line labeled "Crack Initiation Boundary" plays a key role in interpreting the diagram. This line represents the approximate threshold where concrete enters the cracked region; as the diagram moves upward and toward darker colors within this boundary, cracking progresses toward completion. The U-shaped pattern of the crack boundary is fully justifiable, as crack intensity is significantly greater at the beam's center than at the supports. This condition matches the typical bending behavior of simply supported beams with mid-span or distributed loading.

In regions subjected to higher loads (beyond approximately 100 to 150 kilonewtons), nearly the entire beam length enters the cracked phase, dominated by dark brown or red colors. This indicates that the beam has reached the stage of localized failure or global softening, representing a critical performance boundary from a

structural perspective. Such behavior reflects a substantial reduction in stiffness capacity and flexural resistance of the concrete section and holds high significance in structural performance analysis.

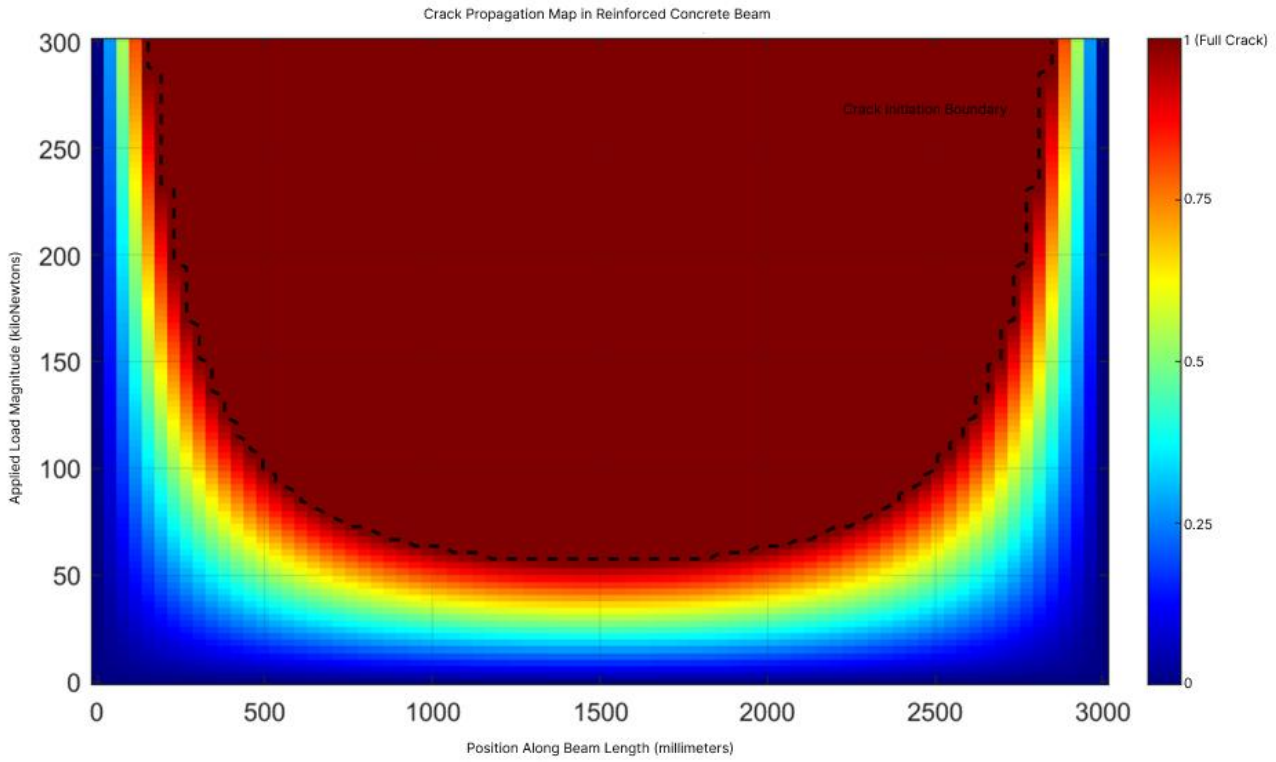

Figure 4. Crack Propagation Map in Reinforced Concrete Beam Section

3.5. Strain Distribution Behavior Along the Section Depth

Figure 5 displays the strain distribution along the depth of the reinforced concrete section, illustrating the linear strain behavior across the section height under flexural loading. The horizontal axis of the diagram represents the strain magnitude (in microstrain or dimensionless units, depending on normalization), and the vertical axis denotes the section height (in millimeters), with the reference origin located at the section's center.

The blue line in the diagram, labeled "Strain Profile," depicts the linear variation of strain along the section height, extending from a negative value at the bottom (e.g., approximately −250 millimeters) to a positive value at the top (+250 millimeters). This behavior is fully consistent with the assumptions of linear flexural theory, which presumes that plane sections remain plane and perpendicular to the neutral axis after bending. Therefore, the strain distribution across the entire section is linear, and the neutral axis lies exactly at the zero strain point, which is identified in the diagram by the vertical dashed black line labeled "Neutral Axis."

The symmetry of the diagram with respect to the central height axis (around y = 0) and the linearity of the strain profile clearly indicate that the section is subjected to pure bending with no axial force. If an axial force were present, the diagram would shift to the left or right, and the neutral axis would no longer coincide with the geometric center. Additionally, the slope of the strain line indicates the curvature of the section, which plays a key role in numerical analyses and flexural capacity design of reinforced concrete sections.

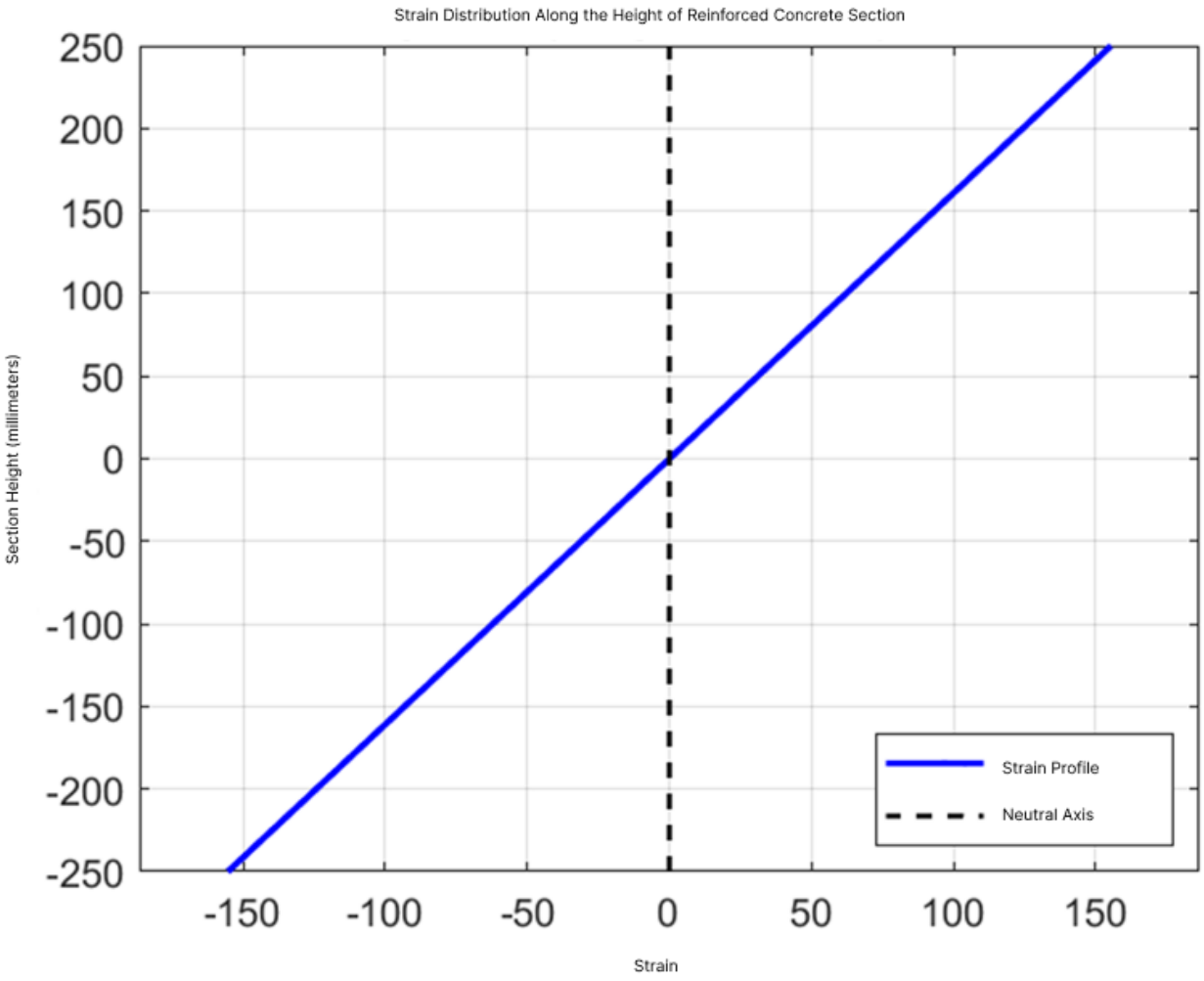

Figure 5. Strain Distribution Along the Depth of Reinforced Concrete Section

3.6. Force–Rotation Performance Evaluation

Figure 6, titled "Moment–Rotation Diagram of Reinforced Concrete Section," is one of the most critical behavioral diagrams in nonlinear analysis and design of reinforced concrete sections, depicting the relationship between bending moment and section rotation under flexural loading. From the perspectives of mechanics of materials and performance-based design, this diagram provides fundamental information regarding flexural capacity, section stiffness or softness, and post-cracking behavior.

In this diagram, the horizontal axis represents section rotation (in milliradians), and the vertical axis shows bending moment (in kilonewton-meters). The thick red line depicts the flexural loading path of the section up to the point of failure. The diagram begins at the origin and reaches a point labeled “Cracking,” marked by a blue circle, where the first behavioral change occurs. This point (known as the concrete cracking point) signifies the moment when the concrete’s tensile zone reaches its tensile strength and begins to crack. At this stage, the concrete’s contribution to tensile stress decreases, and the section’s behavior becomes noticeably more nonlinear.

After this point, the diagram continues with a relatively steep slope and reaches the maximum moment value over a short rotation distance, which is marked by a green circle labeled “Maximum Moment.” This region represents the section’s ultimate flexural capacity, primarily influenced by the yielding of tensile reinforcement and crushing of compressive concrete.

Notably, after reaching this point, the red line continues horizontally, indicating fully plastic behavior—meaning the section can sustain additional deformation (rotation) without any increase in moment. This flat and horizontal behavior

beyond the peak moment point signifies the section's high ductility. Ductility, as a key criterion in seismic design, demonstrates the section's ability to undergo significant deformation prior to complete collapse. The continuation of the diagram without a decrease in moment reflects stable post-yield behavior, which is highly desirable in performance-based design, particularly for structures subjected to cyclic loads such as earthquakes.

In summary, the presented diagram reflects the ideal flexural behavior of a highly ductile reinforced concrete section, in which:

• The elastic region with very high slope appears at the beginning of the diagram.

• The cracking point marks the onset of nonlinear behavior.

• The maximum moment point indicates the section's ultimate flexural capacity.

• The post-yield behavior, maintaining moment with increasing rotation, indicates excellent mechanical durability and ductility.

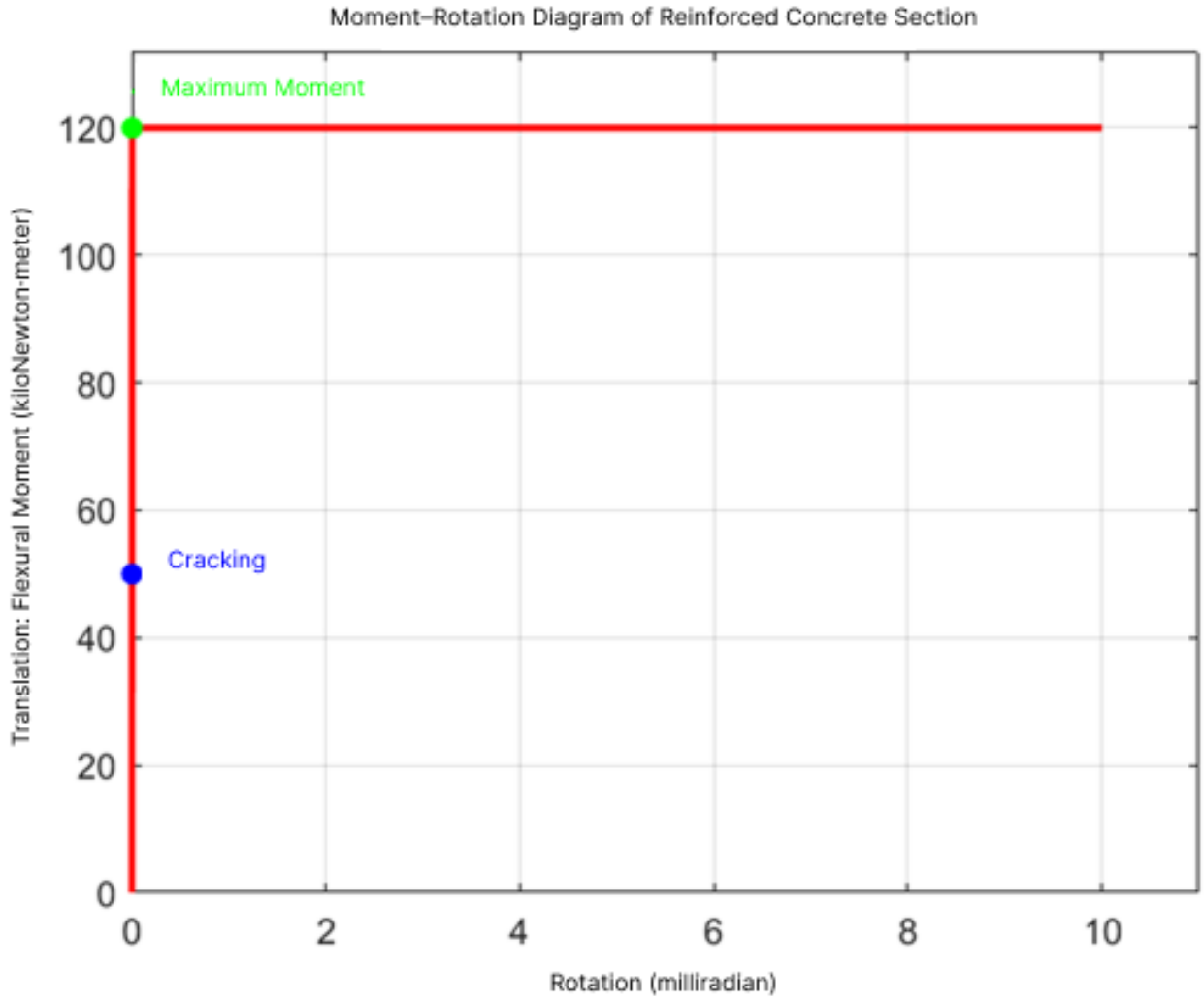

Figure 6. Moment–Rotation Diagram of Reinforced Concrete Section

3.7. Stress Distribution in Reinforcement Bars During Loading

The current diagram, titled "Variation of Rebar Stress under Increasing Bending Moment," is one of the key charts in the behavioral analysis of structural materials, particularly in the nonlinear analysis of reinforced concrete members. This diagram specifically depicts the response of tensile reinforcement bars in a reinforced concrete section under gradually increasing bending moments, enabling analysts to

precisely identify the steel yield point and the linear–nonlinear transition zone in material behavior.

The horizontal axis shows the bending moment in kilonewton-meters, representing the applied flexural loading on the section. The vertical axis displays the rebar stress in megapascals, reflecting the stress level in the tensile steel due to increased bending. The solid blue line, starting from the origin with a defined slope and showing an ascending trend, indicates a linear relationship between increasing bending moment and the induced stress in the rebar. This ascending linear trend in the initial phase reflects that the section is still in the elastic region and stresses in the reinforcement increase according to Hooke's law (i.e., a linear stress–strain relationship). At this stage, both the steel and concrete are in their elastic performance zones, and the overall structural behavior is stable and predictable.

One of the most critical parts of the diagram is the red dashed horizontal line, drawn at a specific stress value (around 400 MPa), which is designated as the yield stress. This line marks the maximum stress that the rebar can endure within the elastic range. Crossing this threshold indicates the onset of the inelastic behavior of steel and entry into the plastic phase, where permanent deformations occur in the reinforcement.

Since the blue line has not yet reached this limit and remains below the red line, it can be concluded that, in this diagram, the rebar has not yet entered the yield zone. In other words, the bending moment has not yet reached the magnitude necessary to yield the tensile reinforcement. This finding indicates that the section is still in the initial performance stage and its ductility capacity has not yet been utilized.

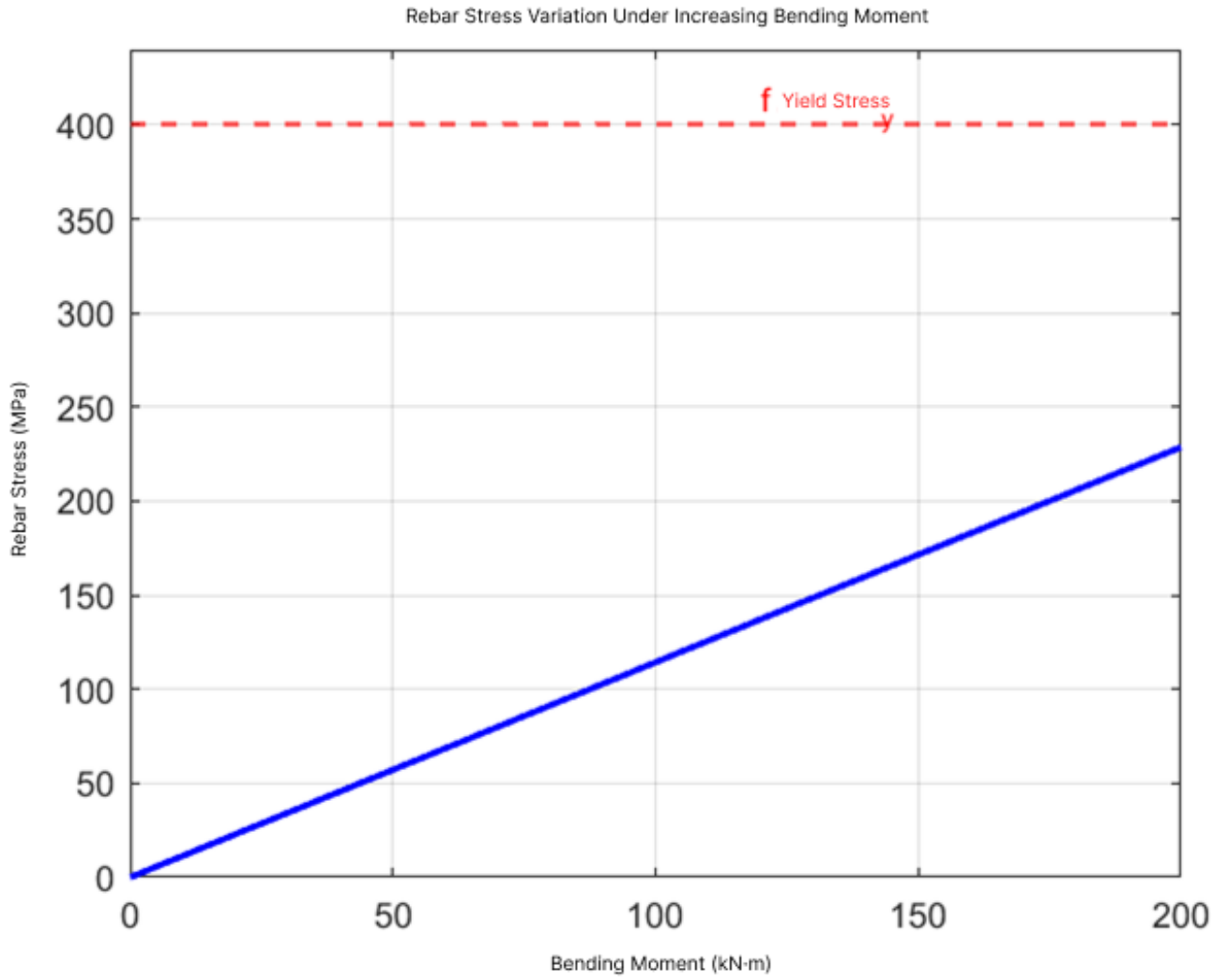

Figure 7. Stress Distribution in Reinforcement Bars During Loading

3.8. Ultimate Load Capacity Surface

Figure 8 presents a three-dimensional diagram that shows the ultimate load-bearing surface of a reinforced concrete section under the combination of axial force and bending moments about the two principal axes. This diagram provides a geometric representation of the ultimate performance domain of the section. That is, combinations of axial load and bending moments lying on or within this surface are sustainable by the section, while combinations outside of it will lead to failure.

The horizontal X-axis represents the bending moment about the X-axis, the horizontal Y-axis represents the moment about the Y-axis, and the vertical Z-axis indicates the compressive axial force. Upon closer inspection of the surface shape, it is evident that the maximum compressive capacity (around 4000 kilonewtons) occurs when both bending moments are zero. This reveals that the member can exhibit its maximum capacity when subjected to pure axial compression, without any flexure.

However, once bending moments are introduced about either axis, the section's ability to resist axial force decreases. This reduction is due to the nonuniform distribution of strain and stress across the cross-section—parts of the concrete enter tension and no longer contribute to load resistance and may even crack. As illustrated in the diagram, increasing either of the moments (about the X or Y axis) causes the surface to bend downward, indicating a decline in the axial load-bearing capacity.

The surface exhibits a convex geometry, and its corners represent critical conditions where specific combinations of bending and compression reach the failure threshold. The color gradient across the surface—from blue to red—visually indicates load-bearing capacity, highlighting safer zones (with warmer colors) and critical zones (with cooler colors).

Overall, this diagram is an extremely useful tool for evaluating the ultimate performance of reinforced concrete sections under combined loading and has wide applications in performance-based design, safety assessment, and nonlinear structural analysis. Any load combination within this surface is considered safe, whereas combinations on or outside the surface indicate conditions at or beyond the member's capacity.

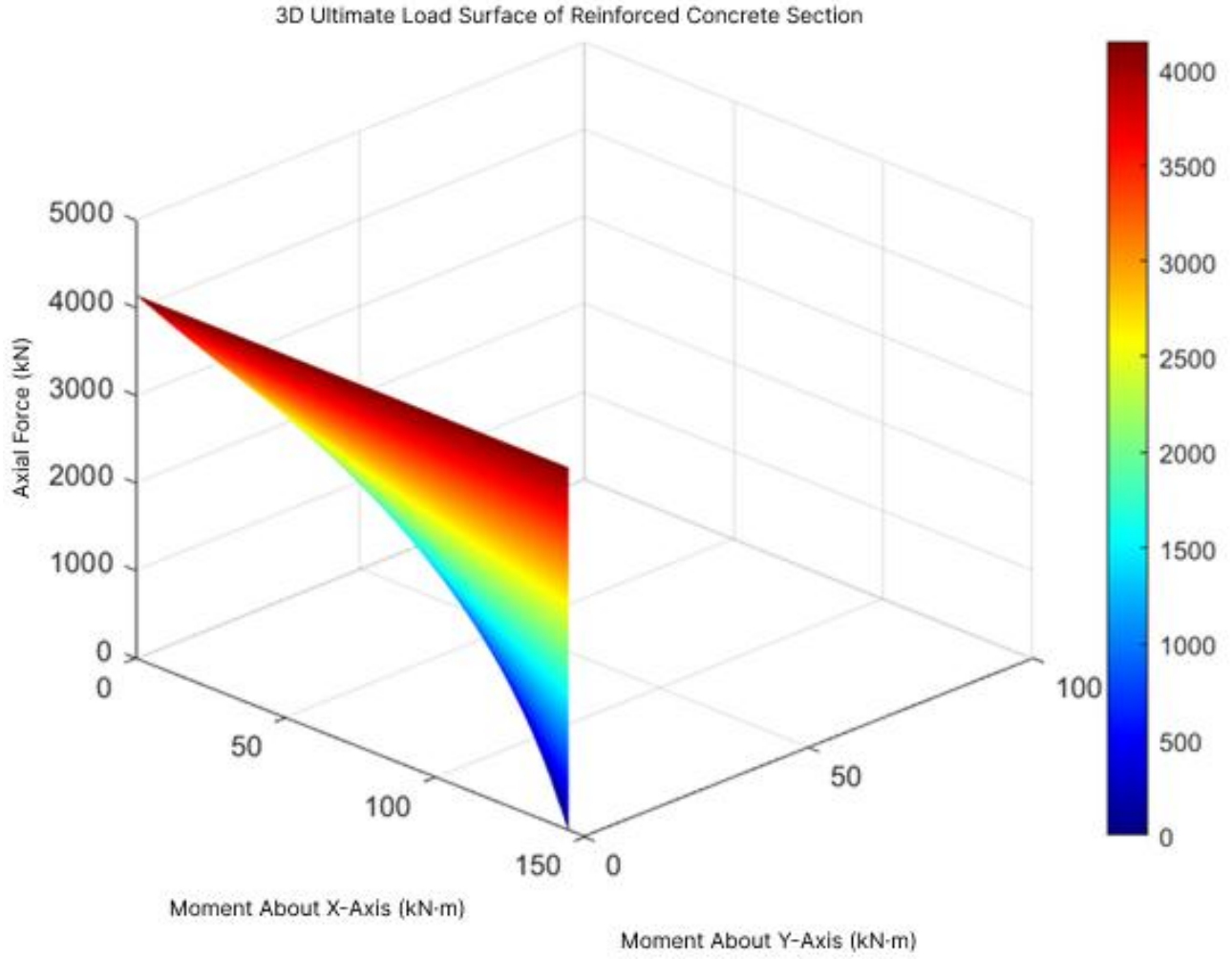

Figure 8. 3D Diagram of the Ultimate Load Capacity Surface of a Reinforced Concrete Section under Combined Axial and Biaxial Bending

3.9. Deformed Shape of the Beam

Figure 9 presents a simply supported beam subjected to a concentrated load at its mid-span. The horizontal axis represents the beam's length in millimeters, and the vertical axis shows the vertical displacement (in the negative direction, i.e., downward), depicted with magnification. The blue curve, labeled "Deformed Shape (Magnified)," illustrates the actual flexural behavior of the beam under loading.

As shown, the maximum displacement occurs at the beam's center—precisely where the concentrated load is applied. This is clearly demonstrated by the symmetry of the curve and the minimum displacement value at the diagram's center. The black dashed line at the top of the diagram represents the initial undeformed shape of the beam. This reference line effectively displays the extent of deviation from the original state due to loading.

The difference between the two curves illustrates the effect of loading and the beam's flexibility. The uniform and symmetric slope on both sides of the curve confirms a linear moment distribution across the two beam halves and the geometric symmetry of the loading condition.

This analysis confirms that the beam behaves in accordance with the predictions of classical bending theory.

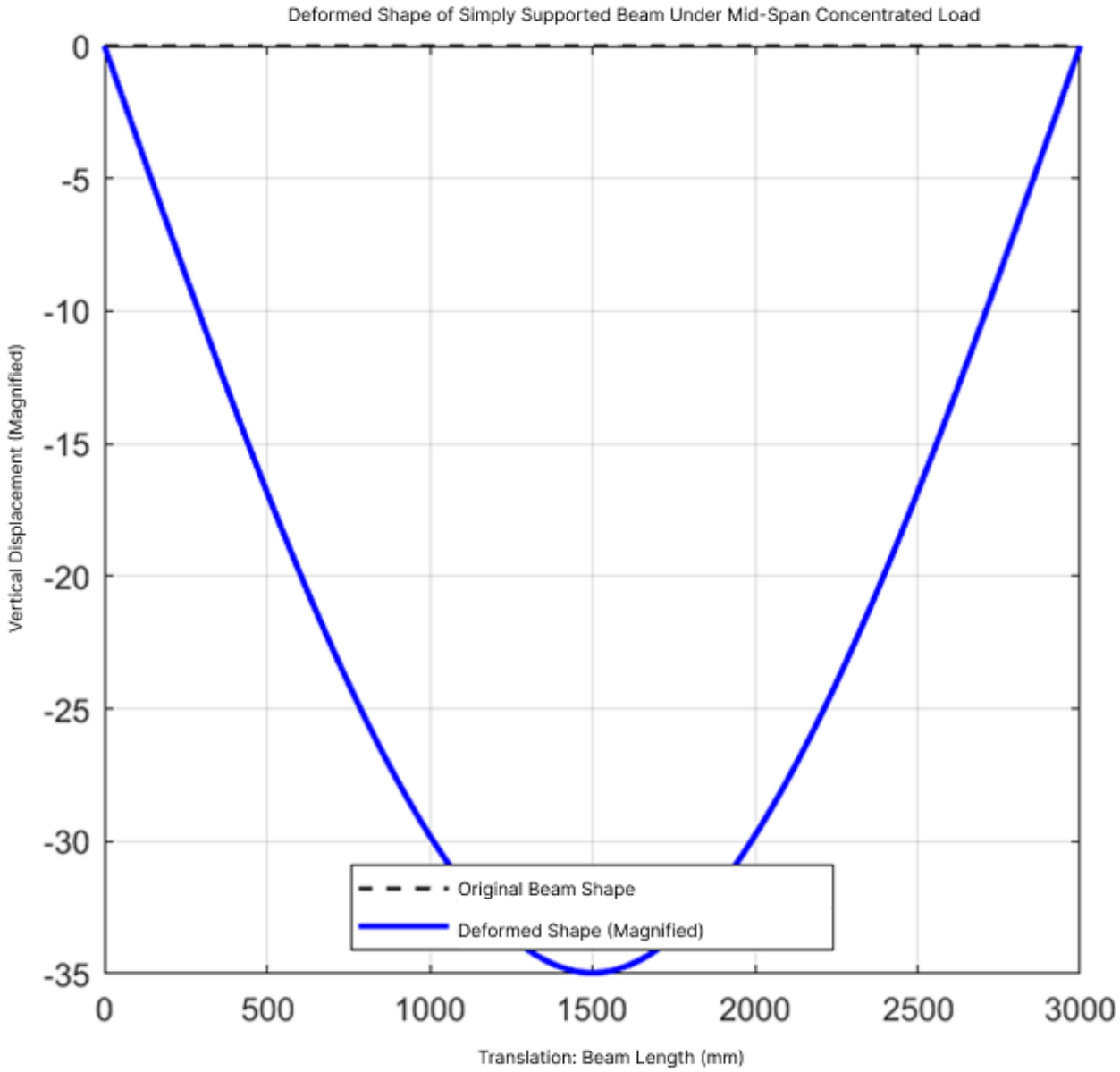

Figure 9. Simply Supported Beam Subjected to a Concentrated Load at Mid-Span

4. Discussion and Conclusion

The findings of the present study provide a comprehensive analysis of the nonlinear flexural and axial behavior of reinforced concrete (RC) beams subjected to combined loading conditions, using MATLAB-based finite element (FE) modeling. The load–displacement curves, moment–curvature responses, axial force–moment interaction surfaces, crack propagation patterns, strain distributions, and rebar stress trajectories collectively offer a holistic understanding of how RC members behave under real-world stress scenarios.

The load–displacement results illustrated a distinct three-phase behavioral response: an initial linear elastic region, a transitional nonlinear stage following concrete cracking, and a post-cracking region characterized by reduced stiffness and increased ductility. This progression aligns closely with prior experimental and numerical studies. For instance, Ali and Umer (2024) documented similar transitions in their study of RC members under combined axial and flexural loading, noting a sharp reduction in stiffness following the initiation of tensile cracking in concrete [6]. Furthermore, the observed displacement increase post-yield, without immediate failure, reflects high ductility, a phenomenon also

emphasized by Musmar (2018) in nonlinear flexural analysis of RC beams [9].

The moment–curvature diagrams generated in the simulations further support the presence of a linear elastic phase followed by a nonlinear softening regime. The curvature continued to increase significantly beyond the peak moment, suggesting sufficient rotation capacity and energy dissipation potential. This trend validates the use of the constitutive plastic-damage models employed in the study, particularly those derived from the frameworks proposed by Lubliner et al. (1989) and refined by Lee and Fenves (1998), which incorporate stiffness degradation and irreversible damage under cyclic and monotonic loads [3, 4].

The stress–strain relationship in the tensile reinforcement bars, as depicted in the stress diagrams, remained within the elastic zone throughout the applied load range, confirming that yielding had not yet occurred. This outcome was consistent with the calculated moment levels, which remained below the theoretical flexural capacity of the section based on Mander's (1983) model for confined concrete [16]. The reinforcement remained in the linear range, supporting the integrity of the section and affirming that the analysis covered the serviceability domain prior to entering the ultimate state.

Crack propagation maps offered valuable visual insights into how damage evolves spatially. Initial cracking was concentrated at the mid-span, correlating precisely with the maximum positive bending moment. As the applied load increased, crack length and intensity expanded symmetrically, consistent with behavior observed in experimental investigations such as those by Jin (2018), who found central flexural cracks to dominate RC beams under impact loading [7]. The graphical depiction of crack evolution in this study, progressing from elastic to plastic zones, is in line with nonlinear fracture mechanics principles and visually reinforces the modeling assumptions made in the simulation framework.

The 3D axial load–biaxial moment interaction surface provided an essential perspective on the member’s ultimate capacity. The surface demonstrated a convex profile, with maximum compressive axial strength recorded when no moments were applied. This interaction behavior reflects classical design expectations and mirrors the analytical models described by Schulz and Santisi D’Avila (2014) using the equivalent section method [19]. It also agrees with the findings by Ponnada and Geddada (2023), who conducted parametric analyses to understand how bending and axial load combinations affect the failure envelope of RC beams [15].

Moreover, the rebar stress response as a function of applied bending moment emphasized the linearity and predictability of steel under moderate loading levels. The rebar stress trajectory did not intersect the yield limit (400 MPa), consistent with the safety margin built into the section design. Such behavior reflects the findings of Contamine (2011), who noted similar stress development in nonlinear models of RC beams under shear and flexural loading [13].

Additionally, the use of MATLAB for implementing the simulation model proved advantageous in terms of adaptability, precision, and post-processing flexibility. The model incorporated damage-based constitutive laws for concrete, embedded reinforcement modeling, and iterative numerical algorithms to simulate the full behavioral spectrum of RC beams. These approaches are directly supported by methodologies in Al-Rumaithi (2025), who developed a nonlinear 3D solver in MATLAB for concrete and steel materials [1]. The flexibility of MATLAB enabled customization of boundary conditions, meshing strategies, and convergence tolerances, echoing previous toolkits introduced by Ishaq (2013) and Papazafeiropoulos (2017) [2, 10].

The accuracy of the simulation results was further supported by the integration of validated material models. The stress–strain relationships applied for concrete, based on Mander (1983) for confined behavior and the cyclic plastic-damage approach of Lee and Fenves (1998), accurately captured the tension stiffening and post-peak softening commonly observed in real structures [4, 16]. The triaxial constitutive laws initially proposed by William and Warnke (1975) also underpin the credibility of the nonlinear material behavior modeling in this study [17].

In line with recent studies, corrosion and deterioration effects were not modeled explicitly in this analysis. However, previous works by Elmezayen et al. (2023) and El Maaddawy et al. (2005) demonstrate how integrating corrosion damage can shift the P-M interaction surface and lower moment capacities significantly [5, 11]. These findings suggest that incorporating deterioration mechanisms in future modeling would enhance realism in long-term performance assessments.

Finally, the graphical representation of the deformed beam shape under central point loading confirmed the symmetrical displacement distribution expected in simply supported beams. The shape of the deflection curve followed classical bending theory, with the maximum deflection at

mid-span and symmetrical gradients toward the supports. This agrees with the theoretical work of Buckhouse (2014) and the simulation-based analysis by Barbosa and Ribeiro (1998), both of whom confirmed the effectiveness of nonlinear FE models in capturing flexural deformation shapes under varied boundary and loading conditions [18, 20].

Despite the depth and accuracy of the analysis, this study presents some limitations. First, the simulation was restricted to static loading conditions and did not consider dynamic, cyclic, or seismic effects, which are essential for evaluating structural performance under real-world loading scenarios. Second, the models assumed perfect bond between concrete and reinforcement, omitting bond-slip effects that can significantly influence behavior, especially near ultimate states. Third, the absence of time-dependent phenomena such as creep, shrinkage, and corrosion may reduce the applicability of the results in long-term durability assessments. Additionally, only a limited number of section geometries and reinforcement layouts were examined, and the mesh density used in some simulations may have affected the accuracy of stress concentrations near supports and load application points.

Future studies should extend the scope of analysis to include dynamic and cyclic loading scenarios, particularly to assess fatigue and seismic performance. Incorporating time-dependent behaviors, such as creep and corrosion progression, would provide more realistic assessments of long-term performance. The use of hybrid modeling strategies that combine finite element methods with machine learning could enhance predictive capacity while reducing computational costs. Moreover, mesh refinement studies, probabilistic modeling, and reliability analysis would strengthen the generalizability of the findings. Investigating more diverse geometries, reinforcement configurations, and boundary conditions would also offer broader applicability in structural design practice.

The outcomes of this research can significantly inform the design and assessment of reinforced concrete beams in practical engineering settings. The simulation framework presented here provides a reliable tool for evaluating service and ultimate performance of RC members under combined loading, supporting both new design and retrofitting projects. Engineers can use the load–displacement and moment–curvature results to optimize reinforcement detailing and ensure adequate ductility. The interaction diagrams and failure surface visualizations offer clear criteria for determining safe load combinations, aiding performance-based design. Finally, the modeling approach developed in MATLAB can be customized for specific project needs, offering flexibility for use in consulting, research, and academic environments.

Authors' Contributions

Authors equally contributed to this article.

Acknowledgments

Authors thank all participants who participate in this study.

Declaration of Interest

The authors report no conflict of interest.

Funding

According to the authors, this article has no financial support.

Ethical Considerations

All procedures performed in this study were under the ethical standards.

References

[1] A. M. Al-Rumaithi, "Nonlinear 3D FE Solver for Steel and Concrete 2. MATLAB Central File Exchange," ed, 2025.
[2] M. Ishaq, *MATLAB toolbox for the design of RC structural members*. 2013.
[3] J. Lubliner, J. Oliver, S. Oller, and E. Oñate, "A plastic-damage model for concrete," *International Journal of Solids and Structures*, vol. 25, no. 3, pp. 299-326, 1989, doi: 10.1016/0020-7683(89)90050-4.
[4] J. Lee and G. L. Fenves, "Plastic-damage model for cyclic loading of concrete structures," *Journal of Engineering Mechanics*, vol. 124, no. 8, pp. 892-900, 1998, doi: 10.1061/(ASCE)0733-9399(1998)124:8(892).
[5] T. El Maaddawy, K. Soudki, and T. Topper, "Analytical model to predict nonlinear flexural behavior of corroded reinforced concrete beams," *ACI structural journal*, vol. 102, no. 4, p. 550, 2005, doi: 10.14359/14559.
[6] S. Ali and M. Umer, "Experimental and Numerical Study on the Behavior of RC Members under Combined LoadsER," ed, 2024.
[7] L. Jin, "Experimental and numerical study of RC beams with steel fibers under impact loading," ed, 2018.
[8] M. K. Effendi, "Non-linear finite element analysis of flexural reinforced concrete beam using embedded reinforcement modeling," Petra Christian University, 2020, vol. 6, 3 ed., p. 271, doi: 10.22146/jcef.55960.
[9] M. Musmar, "Nonlinear finite element flexural analysis of RC beams," *International Journal of Applied Engineering Research*, vol. 13, no. 4, pp. 2014-2020, 2018.

[10] G. Papazafeiropoulos, "Abaqus2Matlab: A suitable tool for finite element post-processing," 2017, doi: 10.1016/j.advengsoft.2017.01.006.
[11] Y. Elmezayen, N. Khattak, and T. El-Maaddawy, "Prediction of nonlinear flexural behavior of continuous rc beams pre-damaged by corrosion," *Buildings*, vol. 13, no. 6, p. 1398, 2023, doi: 10.3390/buildings13061398.
[12] S. Shahbazpanahi and H. F. Hama Ali, "Simulation of shear-strengthening of RC beams by CFRP," ed, 2019.
[13] R. Contamine, "Numerical modeling of reinforced concrete beams under shear stress," ed, 2011.
[14] E. Kantar, "Nonlinear FE analysis of impact behavior of concrete beam," 2011, doi: 10.3390/mca16010183.
[15] M. R. Ponnada and Y. Geddada, "A comprehensive nonlinear finite element modelling and parametric analysis of reinforced concrete beams," ed, 2023.
[16] J. B. Mander, "Theoretical stress-strain model for confined concrete," *Journal of Structural Engineering*, vol. 114, no. 8, pp. 1804-1826, 1983, doi: 10.1061/(ASCE)0733-9445(1988)114:8(1804).
[17] K. J. William and E. P. Warnke, *Constitutive model for the triaxial behavior of concrete*. 1975.
[18] A. F. Barbosa and G. O. Ribeiro, "Analysis of RC structures using ANSYS nonlinear concrete model," ed, 1998.
[19] M. Schulz and M. P. Santisi D'Avila, "Analysis of RC beams by the equivalent section method," ed, 2014.
[20] J. Buckhouse, "Application of nonlinear concrete model for FEA of RC beams," ed, 2014.